ARTICLE
Journal of Cellular Biochemistry 112:2230–2240 (2011)

Journal of Cellular Biochemistry

Differential Carbohydrate Binding and Cell Surface Glycosylation of Human Cancer Cell Lines

Nadia X. Arndt, Joe Tiralongo,* Paul D. Madge, Mark von Itzstein, and Christopher J. Day*

Institute for Glycomics, Gold Coast Campus, Griffith University, Queensland 4222, Australia

ABSTRACT

Currently there is only a modest level knowledge of the glycosylation status of immortalised cell lines that are commonly used in cancer biology as well as their binding affinities to different glycan structures. Through use of glycan and lectin microarray technology, this study has endeavoured to define the different bindings of cell surface carbohydrate structures to glycan-binding lectins. The screening of breast cancer MDA-MB435 cells, cervical cancer HeLa cells and colon cancer Caco-2, HCT116 and HCT116–FM6 cells was conducted to determine their differential bindings to a variety of glycan and lectin structures printed on the array slides. An inverse relationship between the number of glycan structures recognised and the variety of cell surface glycosylation was observed. Of the cell lines tested, it was found that four bound to sialylated structures in initial screening. Secondary screening in the presence of a neuraminidase inhibitor (4-deoxy-4-guanidino-Neu5Ac2en) significantly reduced sialic acid binding. The array technology has proven to be useful in determining the glycosylation signatures of various cell-lines as well as their glycan binding preferences. The findings of this study provide the groundwork for further investigation into the numerous glycan–lectin interactions that are exhibited by immortalised cell lines. J. Cell. Biochem. 112: 2230–2240, 2011.

KEY WORDS: GLYCAN; LECTIN; GLYCOSYLATION; IMMORTALISED CELL LINES; ARRAY

Glycan and lectin arrays are becoming more widely employed as a tool to elucidate the specificity of carbohydrate binding proteins (CBPs), and to evaluate cell surface glycosylation, respectively [Hirabayashi, 2003; Liang et al., 2008; Tao et al., 2008]. Glycosylation is a predominant post-translation modification, with SWISS-PROT estimating that over 50% of all known proteins and lipids synthesised by eukaryotes being glycosylated [Apweiler et al., 1999; Wells and Hart, 2003]. Eukaryotic cells not only possess an extensive repertoire of glycan structures on their cell surface, but also express diverse CBPs (or lectins) that specifically recognise and bind glycan structures on other cells. The interplay between lectins and glycans on neighbouring cells regulates cell–cell communications, and is therefore involved in numerous biological processes including adherence, differentiation, transformation, immunity, and inflammation [Hirabayashi et al., 2002]. Glycan and lectin arrays have been extremely important in assessing glycan–lectin interactions that mediate these processes, providing platforms capable of rapidly producing large quantities of binding data [Tao et al., 2008; Song et al., 2009].

Our interest in better understanding the role of lectin–glycan interactions in malignant transformation lead us to utilise a discrete glycan and lectin array for the analysis of both the glycan bind capacity and cell surface glycosylation of cultured human cancer cells. Aberrant glycosylation is a well-known marker of malignant transformation and tumour progression [Cornil et al., 1990; Iozzo and Cohen, 1993; Dennis et al., 1999; Hakomori, 2002], and even though cultured human cancer cells are frequently used as models in cancer research and cell biology in general, little is known about the extent and nature of glycosylation present on, and the glycan structures recognised by, these commonly used cell lines. Here we describe the systematic Glycomics evaluation of five human cancer cell lines (HCT116, HCT116–FM6 (expressing MUC1), MDA-MB435, HeLa and Caco-2 cells) frequently used as models in cancer and cell biology research using glycan and lectin arrays.

MATERIALS AND METHODS

PREPARATION OF GLYCAN AND LECTIN ARRAYS

Glycans sourced from Dextra Laboratories (Reading, UK) and Glycoseparations (Moscow, Russia) were functionalised and printed on activated SuperEpoxy 2 glass slides (ArrayIt Microarray Technologies, Sunnyvale, CA) as previously described [Day et al., 2009]. Two identical sub-arrays consisting of 120 glycans printed in

Additional supporting information may be found in the online version of this article.

*Correspondence to: Joe Tiralongo or Christopher J. Day, Institute for Glycomics, Gold Coast Campus, Griffith University, Queensland 4222, Australia. E-mail: j.tiralongo@griffith.edu.au or c.day@griffith.edu.au

Received 17 February 2011; Accepted 31 March 2011 • DOI 10.1002/jcb.23139 • © 2011 Wiley-Liss, Inc.
Published online 7 April 2011 in Wiley Online Library (wileyonlinelibrary.com).

replicates of four were prepared per slide. A full list of glycans printed is given in Table I.

Lectins obtained from EY Laboratories (San Mateo, CA) and Sigma-Aldrich, St. Louis, MO were directly printed onto SuperEpoxy 2 glass slides without modification and blocked as described by [Hartley-Tassell et al., 2010]. Four identical sub-arrays consisting of 18 lectins printed in replicates of three were prepared per slide.

CULTURING, HARVESTING AND FLUORESCENT LABELLING OF HUMAN CANCER CELL LINES

The human cancer cell lines used in this study (Table II) were cultured in minimum essential medium (MEM) supplemented with 10% foetal calf serum (Life Technologies, Carlsbad, CA), 100 μg/ml penicillin, 100 μg/ml streptomycin, 2 mM glutamine and 10% sodium pyruvate. Cells were allowed to grow at 37°C in a humidified incubator with 5% CO_2 until they had reached greater than 80% confluence. Cells were harvested by cell-scraping and collected by centrifugation at 1,200 rpm for 5 min. The resulting pellet was washed 4–5 times with warmed PBS, pH 7.4, resuspended in 0.5–1 ml CFDA-SE (Carboxyfluorescein diacetate succinimidyl ester; Invitrogen, Mount Waverly, Victoria) 25 μM in PBS at 10^6 cells/ml and incubated for 30–60 min on ice. Cells were subsequently pelleted and visually inspected for staining of cells by fluorescence microscopy. Stained cells were washed three times in PBS, three times in MEM media and resuspended at the required cell concentration in the required volume (125 μl for each glycan sub-array, and 65 μl for each lectin sub-array).

Prior to application of cells to glycan and lectin arrays, each CFDA-labelled cell line was assessed for the extent and level of fluorescence by flow cytometric analysis using a Becton Dickinson FACSCalibur flow cytometer and CellQuest software (Becton Dickson, Franklin Lakes, NJ Immunocytometry Systems). Labelled cells (2.5×10^5) were suspended in 500 μl of 1% formaldehyde and 0.05% BSA in PBS, and fluorescence detected using the 488 nm laser where auto-fluorescence was initially determined by measuring cells that were untreated with CFDA-SE.

APPLICATION TO GLYCAN AND LECTIN ARRAYS

Each of the glycan and lectin sub-arrays present per slide was isolated using a 1.7×2.8 cm (125 μl) and 1.5×1.6 cm (65 μl) Gene Frame (Abgene, Epsom, UK), respectively, into which 10^5–10^6 CFDA-labelled cells was added. Each sub-array was covered with a GeneFrame coverslip (Abgene) and incubated in the dark for 15–30 min in a humidified incubator at 37°C. GeneFrames and coverslips were then removed and the slides carefully washed with 50 ml of pre-warmed PBS containing 1 mM Mg^{2+} and 1 mM Ca^{2+} by gently flowing 1 ml at a time across the surface of the array. Glycan arrays were also performed with the addition of the influenza virus sialidase inhibitor 4-deoxy-4-guanidino-Neu5Ac2en to a final concentration of 1 mM to inhibit cell surface Neu3 [Hata et al., 2008]. Slides were then fixed by incubation in 10% formaldehyde/PBS solution in a 50 ml tube for 5 min. Following washing with PBS, slides were dried by centrifugation at 900 rpm for 3 min in 50 ml.

FLUORESCENT IMAGE ACQUISITION AND DATA PROCESSING

Fluorescence intensities of the array spots were measured using the ProScanArray Microarray 4-laser scanner (Perkin Elmer, Waltham, MA) using the Blue Argon 488 excitation laser set to the FITC setting (492 nm excitation and 517 nm emission). Image analysis was carried out using the ProScanArray imaging software, ScanArray Express (Perkin Elmer). Statistical analysis was performed using Microsoft EXCEL software by performing independent sample *T*-tests.

DETERMINATION OF RELATIVE FLUORESCENCE

The extent and level of fluorescent labelling of each cell line as determined by flow cytometric analysis was used to generate a relative fluorescence normalisation value (N_F). This value was used to normalise each cell line with respect to the percentage of cells labelled and the level of labelling. The equation used to generate N_F is given by the following formula: $N_F = \frac{\left(L_{\bar{x}} \times 10^{-2}\right)^{-1}}{F_{\bar{x}} \times 10^{-3}}$ where $L_{\bar{x}}$ is the mean percentage of cells labelled with CFDA, and $F_{\bar{x}}$ is the mean level of fluorescence associated with the cells.

RESULTS

FLOW CYTOMETRIC ANALYSIS OF CFDA-LABELLED CELLS

Flow cytometric analysis of CFDA-labelled cells (Fig. 1, Supplementary Material) showed that each cell line stained differently with respect to cell number and level of fluorescence. Table III shows that the percentage of HeLa cells labelled with CFDA is considerably lower than other cell lines tested. Conversely, the level of fluorescence associated with Caco-2 CFDA-labelled cells was almost double that on other cells. Therefore, in order to appropriately compare glycan and lectin array data between cell lines, a fluorescence correction or normalisation factor (N_F) was determined (Table III) and applied to raw fluorescence intensities obtained following array hybridisation.

GLYCAN ARRAY ANALYSIS

Glycan array experiments were performed in order to elucidate the glycan binding specificities of five cell lines (Table II) commonly used as in vitro models in cancer and cell biology studies. Each cell line was grown under optimum cell culturing conditions, labelled with the fluorescent dye CFDA and applied to our glycan array at between 10^5–10^6 cells per sub-array. Interactions of labelled cells with immobilised glycans were verified both manually through visual inspection of scanned images and through statistical analysis, with only statistically significant ($P < 0.05$) binding to glycans over background being considered a positive interaction. For simplicity the glycans present on our array have been grouped in six major classes: those containing terminal galactose (Gal; 24 members), those containing terminal *N*-acetylglucosamine (GlcNAc; 5 members), mannosylated glycans (8 members), fucosylated glycans (33 members), sialylated glycans (20 members) and glycosaminoglycans (GAGs) and related structures (42 members). Significant differential binding of human cultured cancer cells was observed in all six classes of glycan structures present on our glycan array.

To the best of our knowledge, none of the cultured cells used in this study have been assessed for carbohydrate binding potential by

TABLE I. Glycan Structures Present on Array

Class	Glycan	ID
Terminal Galactose	Galβ1-3GlcNAc	1A
	Galβ1-4GlcNAc	1B
	Galβ1-4Gal	1C
	Galβ1-6GlcNAc	1D
	Galβ1-3GalNAc	1E
	Galβ1-3GalNAcβ1-4Galβ1-4Glc	1F
	Galβ1-3GlcNAcβ1-3Galβ1-4Glc	1G
	Galβ1-4GlcNAcβ1-3Galβ1-4Glc	1H
	Galβ1-4GlcNAcβ1-6(Galβ1-4GlcNAcβ1-3)Galβ1-4Glc	1I
	Galβ1-4GlcNAcβ1-6(Galβ1-3GlcNAcβ1-3)Galβ1-4Glc	1J
	Galα1-4Galβ1-4Glc	1K
	GalNAcα1-O-Ser	1L
	Galβ1-3GalNAcα1-O-Ser	1M
	Galα1-3Gal	1N
	Galα1-3Galβ1-4GlcNAc	1O
	Galα1-3Galβ1-4Glc	1P
	Galα1-3Galβ1-4Galα1-3Gal	2A
	Galβ1-6Gal	2B
	GalNAcβ1-3Gal	2C
	GalNAcβ1-4Gal	2D
	Galα1-4Galβ1-4GlcNAc	2E
	GalNAcα1-3Galβ1-4Glc	2F
	Galβ1-4GlcNAcβ1-6(Galβ1-4GlcNAcβ1-3)Galβ1-4Glc	2G
	Galβ1-3GlcNAcβ1-3Galβ1-4GlcNAcβ1-6(Galβ1-3GlcNAcβ1-3)Galβ1-4Glc	2H
N-Acetylglucosamine	GlcNAcβ1-4GlcNAc	4A
	GlcNAcβ1-4GlcNAcβ1-4GlcNAc	4B
	GlcNAcβ1-4GlcNAcβ1-4GlcNAcβ1-4GlcNAc	4C
	GlcNAcβ1-4GlcNAcβ1-4GlcNAcβ1-4GlcNAcβ1-4GlcNAcβ1-4GlcNAc	4D
	GlcNAcβ1-4MurNAc	4E
Mannosylated	GlcNAcβ1-2Man	5A
	GlcNAcβ1-2Manα1-6(GlcNAcβ1-2Manα1-3)Man	5B
	Manα1-2Man	5C
	Manα1-3Man	5D
	Manα1-4Man	5E
	Manα1-6Man	5F
	Manα1-6(Manα1-3)Man	5G
	Manα1-6(Manα1-3)Manα1-6(Manα1-3)Man	5H
Fucosylated	Fucα1-2Galβ1-3GlcNAcβ1-3Galβ1-4Glc	7A
	Galβ1-3(Fucα1-4)GlcNAcβ1-3Galβ1-4Glc	7B
	Galβ1-4(Fucα1-3)GlcNAcβ1-3Galβ1-4Glc	7C
	Fucα1-2Galβ1-3(Fucα1-4)GlcNAcβ1-3Galβ1-4Glc	7D
	Galβ1-3(Fucα1-4)GlcNAcβ1-3Galβ1-4(Fucα1-3)Glc	7E
	Fucα1-2Gal	7F
	Fucα1-2Galβ1-4Glc	7G
	Galβ1-4(Fucα1-3)Glc	7H
	Galβ1-4(Fucα1-3)GlcNAc	7I
	Galβ1-3(Fucα1-4)GlcNAc	7J
	GalNAcα1-3(Fucα1-2)Gal	7K
	Fucα1-2Galβ1-4(Fucα1-3)Glc	7L
	Galβ1-3(Fucα1-2)Gal	7M
	Fucα1-2Galβ1-4(Fucα1-3)GlcNAc	7N
	Fucα1-2Galβ1-3GlcNAc	7O
	Fucα1-2Galβ1-3(Fucα1-4)GlcNAc	7P
	SO3-3Galβ1-3(Fucα1-4)GlcNAc	8A
	SO3-3Galβ1-4(Fucα1-3)GlcNAc	8B
	Galβ1-3GlcNAcβ1-3Galβ1-4(Fucα1-3)GlcNAcβ1-3Galβ1-4Glc	8C
	Galβ1-4(Fucα1-3)GlcNAcβ1-6(Galβ1-3GlcNAcβ1-3)Galβ1-4Glc	8D
	Galβ1-4(Fucα1-3)GlcNAcβ1-6(Fucα1-2Galβ1-3GlcNAcβ1-3)Galβ1-4Glc	8E
	Galβ1-4(Fucα1-3)GlcNAcβ1-6(Fucα1-2Galβ1-3(Fucα1-4)GlcNAcβ1-3)Galβ1-4Glc	8F
	Galβ1-4GlcNAcβ1-3Galβ1-4(Fucα1-3)Glc	8G
	Fucα1-2Galβ1-4(Fucα1-3)GlcNAcβ1-3Galβ1-4Glc	8H
	Fucα1-3Galβ1-4GlcNAcβ1-3Galβ1-4(Fucα1-3)Glc	8I
	Fucα1-2Galβ1-4(Fucα1-3)GlcNAcβ1-3(Fucα1-2)Galβ1-4Glc	8J
	Galβ1-4(Fucα1-3)GlcNAcβ1-6(Galβ1-4GlcNAcβ1-3)Galβ1-4Glc	8K
	Galβ1-4(Fucα1-3)GlcNAcβ1-6(Galβ1-4(Fucα1-3)GlcNAcβ1-3)Galβ1-4Glc	8L
	Fucα1-2Galβ1-4(Fucα1-3)GlcNAcβ1-6(Galβ1-4GlcNAcβ1-3)Galβ1-4Glc	8M
	Galβ1-3GlcNAcβ1-3Galβ1-4(Fucα1-3)GlcNAcβ1-6(Galβ1-3GlcNAcβ1-3)Galβ1-4Glc	8N
	Fucα1-2Galβ1-3GlcNAcβ1-3Galβ1-4(Fucα1-3)GlcNAcβ1-6(Galβ1-3GlcNAcβ1-3)Galβ1-4Glc	8O
	GalNAcβ1-3(Fucα1-2)Galβ1-4Glc	8P
	Galβ1-3(Fucα1-2)Galβ1-4(Fucα1-3)Glc	9A
Sialylated	Neu5Acα2-3Galβ1-3(Fucα1-4)GlcNAc	10A
	Neu5Acα2-3Galβ1-4(Fucα1-3)GlcNAc	10B
	Neu5Acα2-3Galβ1-3GlcNAcβ1-3Galβ1-4Glc	10C
	Galβ1-4(Fucα1-3)GlcNAcβ1-6(Neu5Acα2-6Galβ1-4GlcNAcβ1-3)Galβ1-4Glc	10D

(Continues)

TABLE I. (*Continued*)

Class	Glycan	ID
	Neu5Acα2-3Galβ1-3(Neu5Acα2-6)GalNAc	10E
	Fucα1-2Galβ1-3(Neu5Acα2-6)GlcNAcβ1-3Galβ1-4Glc	10F
	Neu5Acα2-3Galβ1-3(Fucα1-4)GlcNAcβ1-3Galβ1-4Glc	10G
	Neu5Acα2-6Galβ1-3GlcNAcβ1-3Galβ1-4(Fucα1-3)Glc	10H
	Neu5Acα2-6Galβ1-4GlcNAcβ1-6(Galβ1-3GlcNAcβ1-3)Galβ1-4Glc	10I
	Galβ1-4GlcNAcβ1-6(Neu5Acα2-6Galβ1-4GlcNAcβ1-3)Galβ1-4Glc	10J
	Neu5Acα2-3Galβ1-4GlcNAc	10K
	Neu5Acα2-6Galβ1-4GlcNAc	10L
	Neu5Acα2-3Galβ1-3GlcNAcβ1-3Galβ1-4Glc	10M
	Galβ1-3(Neu5Acα2-6)GlcNAcβ1-3Galβ1-4Glc	10N
	Neu5Acα2-6Galβ1-4GlcNAcβ1-3Galβ1-4Glc	10O
	Neu5Acα2-3Galβ1-3(Neu5Acα2-6)GlcNAcβ1-3Galβ1-4Glc	10P
	Neu5Acα2-3Galβ1-4Glc	11A
	Neu5Acα2-6Galβ1-4Glc	11B
	(Neu5Acα2-8Neu5Ac)n	11C
	(Neu5Acα2-6Galβ1-4GlcNAcβ1-2Manα1-6)2Manβ1-4GlcNAcβ1-4GlcNAc-Asn	11D
GAGs and related structures	Neocarratetraose-41, 3-di-*O*-sulphate (Na^+)	12A
	Neocarratetraose-41-*O*-sulphate (Na^+)	12B
	Neocarrahexaose-24,41, 3, 5-tetra-*O*-sulphate (Na^+)	12C
	Neocarrahexaose-41, 3, 5-tri-*O*-sulphate (Na^+)	12D
	Neocarraoctaose-41, 3, 5, 7-tetra-*O*-sulphate (Na^+)	12E
	Neocarradecaose-41, 3, 5, 7, 9-penta-*O*-sulphate (Na^+)	12F
	ΔUA-2S→GlcNS-6S Na_4 (I-S)	12G
	ΔUA→GlucNS-6S Na3 (II-S)	12H
	ΔUA→2S-GlcNS Na_3 (III-S)	12I
	ΔUA→2S-GlcNAc-6S Na_3 (I-A)	12J
	ΔUA→GlcNAc-6S Na_2 (II-A)	12K
	ΔUA→2S-GlcNAc Na_2 (III-A)	12L
	ΔUA→GlcNAc Na (IV-A)	12M
	ΔUA→GalNAc-4S Na_2 (Δ Di-4S)	12N
	ΔUA→GalNAc-6S Na_2 (Δ Di-6S)	12O
	ΔUA→GalNAc-4S,6S Na_3 (Δ Di-disE)	12P
	ΔUA→2S-GalNAc-4S Na_2 (Δ Di-disB	13A
	ΔUA→2S-GalNAc-6S Na_3 (Δ Di-disD)	13B
	ΔUA→2S-GalNAc-4S-6S Na_4 (Δ Di-tisS)	13C
	ΔUA→2S-GalNAc-6S Na_2 (Δ Di-UA2S)	13D
	ΔUA→GlcNAc Na (Δ Di-HA)	13E
	$(GlcAb1\text{-}3GlcNAcb1\text{-}4)_n$ (n = 4)	13F
	$(GlcAb1\text{-}3GlcNAcb1\text{-}4)_n$ (n = 8)	13G
	$(GlcAb1\text{-}3GlcNAcb1\text{-}4)_n$ (n = 10)	13H
	$(GlcAb1\text{-}3GlcNAcb1\text{-}4)_n$ (n = 12)	13I
	$(GlcA/IdoAa/b1\text{-}4GlcNAca1\text{-}4)_n$ (n = 200)	13J
	$(GlcA/IdoAb1\text{-}3(\pm4/6S)GalNAcb1\text{-}4)_n$ (n < 250)	13K
	$((\pm2S)GlcA/IdoAa/b1\text{-}3(\pm4S)GalNAcb1\text{-}4)_n$ (n < 250)	13L
	$(GlcA/IdoAb1\text{-}3(\pm6S)GalNAcb1\text{-}4)_n$ (n < 250)	13M
	HA-4 10 mM	13N
	HA-6 10 mM	13O
	HA-8 9.7 mM	13P
	HA-10 7.83 mM	14A
	HA-12 6.5 mM	14B
	HA-14 5.6 mM	14C
	HA-16 4.9 mM	14D
	HA 30,000 Da 2.5 mg/ml	14E
	HA 107,000 Da 2.5 mg/ml	14F
	HA 190,000 Da 2.5 mg/ml	14G
	HA 222,000 Da 2.5 mg/ml	14H
	HA 1,600,000 Da 2.5 mg/ml	14I

glycan array analysis previously. Significant binding observed for each of the cell lines to glycans present on the array are presented in Figure 1 (interactions deemed significant indicated by red shading).

Caco-2 are heterogeneous human epithelial colorectal adenocarcinoma cells commonly used as a model of the human small intestinal mucosa and as such are employed in diverse cell-based assays, including bacterial adhesion, transwell migration and pharmacokinetics/drug absorption studies. Figure 1 shows that Caco-2 cells were able to only weakly interact with 16 glycans on our array, with relative background subtracted fluorescence

TABLE II. Human Cancer Cell Lines Evaluated by Glycan and Lectin Array in This Study

Cell line	ATCC No.	Cancer type	Morphology	Reference
HeLa	CCL-2	Cervical carcinoma	Epithelial	Jones et al. [1971]
HCT116	CCL-247	Colorectal carcinoma	Epithelial	Brattain et al. [1981]
HCT116–FM6	–	Colorectal carcinoma expressing MUC1	Epithelial	McAuley et al. [2007]
Caco-2	HTB-37	Colorectal adenocarcinoma	Polarised, Epithelial	Jumarie and Malo [1991]
MDA-MB435	HTB-129	Ductal breast carcinoma	Spindle shaped	Cailleau et al. [1978]

TABLE III. Summary of Data Generated From Flow Cytometry Analysis of Cell Lines Stained With CFDA. A Normalisation Factor (N_F) was Determined for Each Cell Line as Described Under Materials and Methods Section Prior to Glycan and Lectin Array Analysis

Cell line	Mean % labelled ± SD	Mean fluorescence ± SD	N_F
HCT116	99.34 ± 0.372	2466.53 ± 209.926	0.40812
HCT116–FM6	98.88 ± 0.047	2312.12 ± 171.799	0.43738
HeLa	68.77 ± 1.720	2208.65 ± 281.169	0.65841
MDA-MB435	97.40 ± 0.288	3815.99 ± 52.308	0.26906
Caco-2	90.62 ± 0.361	4648.88 ± 81.169	0.23738

intensities below 250 FU (Fig. 2, Supplementary Material). Of these 11 glycans the majority of interactions were clustered around two classes of glycan, with binding observed to four oligo-mannose structures (5B, 5C, 5D, and 5H), and hyaluronan fragments of varying lengths (13N, 13O, and 14A–14E). Note that Caco-2 cells did not interact with any of the sialylated glycans present on our array.

HCT116 are epithelial colorectal carcinoma cells commonly used in cell based binding assays including bacterial adherence. HCT116 cells interacted with 24 glycans on our array with relative fluorescence intensities above 250 FU (Fig. 3, Supplementary Material). Similar to that observed with Caco-2 cells, HCT116 interactions clustered around oligo-mannose structures, and hyaluronan fragments, but also numerous fucosylated glycans were also bound by HCT116 cells (7A, 7C, 7G, 7P, 8D, and 8E). HCT116 cells also bound two sialylated structures (10A, 10D) (Fig. 1).

The MUC-1-expressing HCT116–FM6 cell line was also assessed on our glycan array. Interestingly not only were the total number of glycans bound by this cell line (36 glycans, Fig. 1) greater than that observed for wild-type HCT116 counterpart, but also the level of binding as determined from relative fluorescence intensities was also increased (Fig. 4, Supplementary Material). In comparison to HCT116, HCT116–FM6 bound a greater number of terminal galactose (1B, 1C, 1D and 2A), fucosylated (7A, 7C, 7F–I, 7K, 7N, 7P, 8D, 8E and 8G) and sialylated (10A, 10L, 10N, and 10P) glycans, as well as binding two *N*-acetylglucosamine (GlcNAc) structures (4B and 4E). HCT116–FM6 also bound the same hyaluronan fragments recognised by HCT116 cells (Fig. 1).

Glycan array screening of cervical cancer HeLa cells revealed novel binding to a total of 49 glycan structures (Fig. 1) with high relative fluorescence intensities (Fig. 5, Supplementary Material). Similar to the other cell lines assessed, positive interactions were clustered around oligo-mannose and fucosylated structures, as well as hyaluronan fragments, with additional interactions observed to various carrageenan oligosaccharides (12A–12F) and an extended number of GAG fragments. Also noteworthy was the lack of binding to GlcNAc structures, in fact HeLa cells were the only cell line that did not bind to at least one poly-GlcNAc glycan. HeLa cells also interacted with five sialylated glycans (10L, 10N–P, 11B), however no linkage specificity was observed.

MDA-MB435 cells have historically been used as a common model of ductal breast carcinoma, however the exact nature of this cell line has been brought into question since analysis of DNA microarray data suggested that they might be of melanocyte origin [Ross et al., 2000]. Our evaluation showed that MDA-MB435 cells bound the broadest number of glycans, with 52 structures recognised (Fig. 1) at relative fluorescence intensities similar to that seen for HCT116–FM6 and HeLa cells (Fig. 6, Supplementary Material). MDA-MB435 was able to bind member structures in each of the six classes of glycans present on our array, including the largest subset of terminal galactose (1B, 1F–1I, 2C, 2F) and sialylated glycans (10A–C, 10L–N, 10P, 11A) compared to other cell lines evaluated.

In our initial glycan array analysis binding to sialylated structures was observed for all cell lines except for Caco-2 cells, which did not bind to any of the 20 sialylated glycans present on our array. These cell lines were able to bind both α-2,3 and α-2,6 linked Sia, thus exhibiting no linkage specificity. As cancer cell lines are not know for their sialic acid binding potential, but do express a plasma membrane sialidase Neu3 [Kakugawa et al., 2002; Miyagi et al., 2008], glycan array experiments were also performed in the presence of the influenza sialidase inhibitor 4-deoxy-4-guanidino-Neu5Ac2en [Hata et al., 2008]. Figure 2 and Supplementary Material Figures 7–10 clearly show that in the presence of sialidase inhibitor all Sia binding was eliminated, with the exception of weak binding of MDA-MB435 cells to sialyl-lewis A (10A). This strongly indicates that in the absence of sialidase inhibitor, Neu3 removed the terminal Sia from sialylated glycans present on our array exposing the sub-terminal sugar, Gal, which were subsequently bound by the cells evaluated. This is further supported by the observation that Caco-2 cells did not bind terminal Gal structures on the array, or sialylated structures in the absence of the inhibitor (exposed sub-terminal Gal).

LECTIN ARRAY ANALYSIS

Lectin array screening was conducted to determine the glycosylation profile of the same five human cancer cell lines assessed by the glycan array. Each cell line was CFDA labelled and applied to our lectin array at between 10^5–10^6 cells per sub-array. Interactions of labelled cells with immobilised lectins were verified both manually through visual inspection of scanned images and through statistical analysis, with only statistically significant ($P < 0.05$) binding to lectins over background being considered as positive. Figure 3 summarises our lectin array data, with interactions deemed significant indicated by red shading.

Caco-2 cells exhibited significant binding to numerous immobilised lectins, with the highest relative fluorescence intensities observed to ECA, LFA, and WGA that suggests the presence of LacNAc (Galβ(1,4)GlcNAc), Sia and/or GlcNAc containing glycoconjugates, respectively (Fig. 11, Supplementary Material). Branched mannosylated structures, identified through ConA binding, were also detected, as well as terminal α-Gal/α-GalNAc-containing structures (MPA binding). Very weak binding to 1 mg/ml immobilised UEA and SJA was observed suggesting the presence of fucosylated and β-GalNAc-containing glycoconjugates. All significant Caco-2 interactions on our array were dependent on the concentration of lectin printed, with the exception of ABA (recognises β-Gal) and anti-GM1, which were only bound at 250 μg/ml (lowest concentration printed). This suggests that

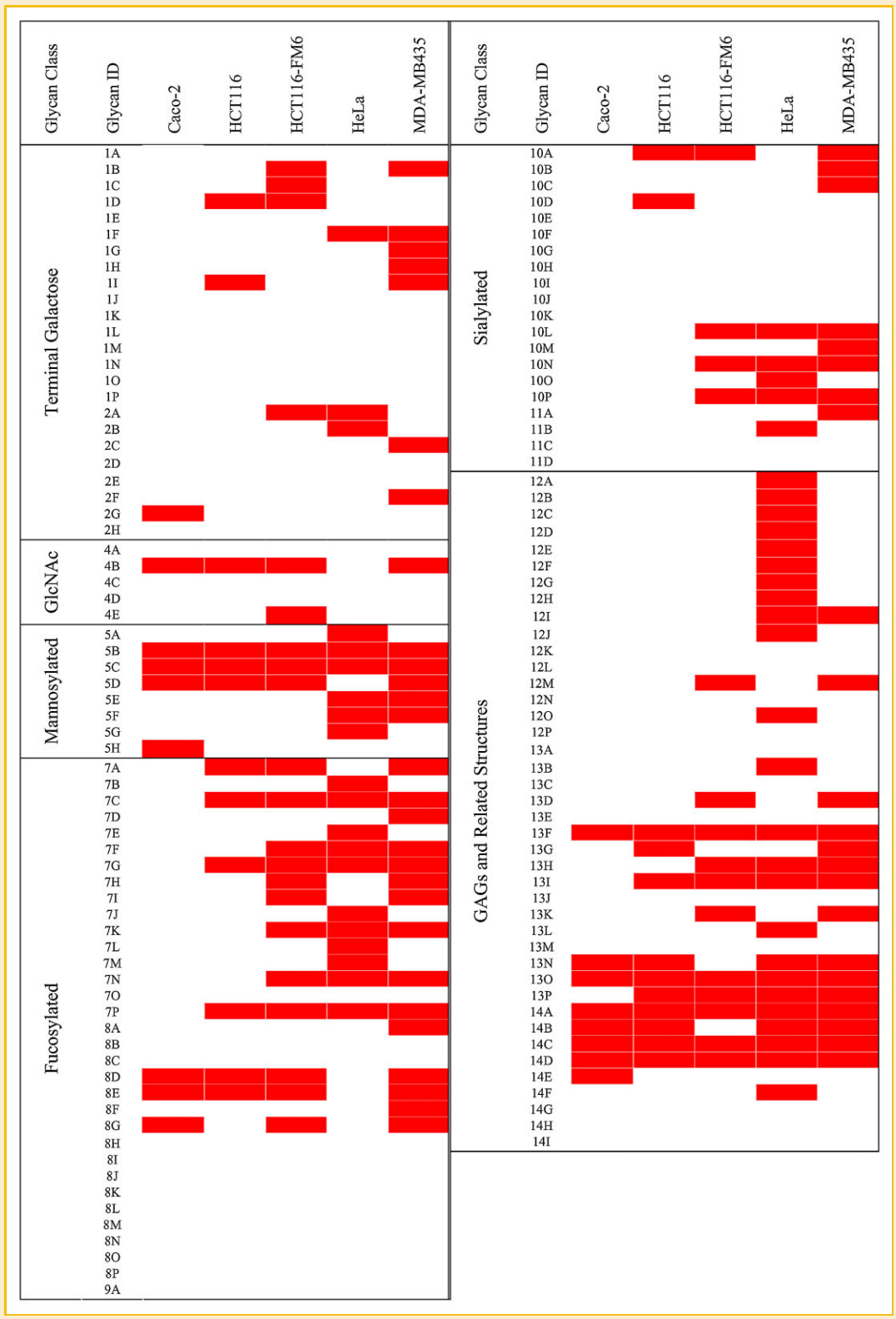

Fig. 1. Summary of significant glycan binding interactions for five cultured human cancer cell lines as assessed by glycan array analysis.

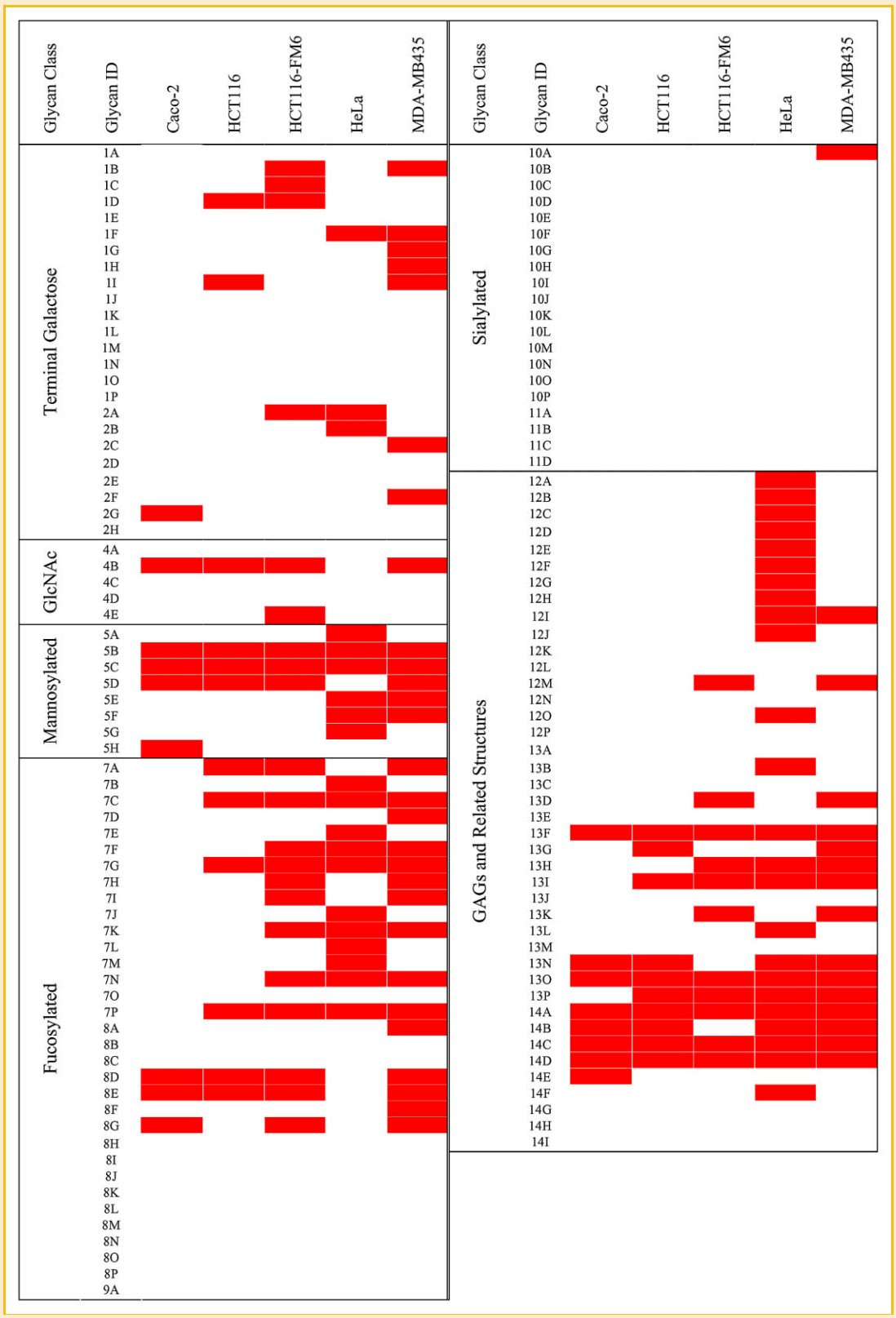

Fig. 2. Summary of significant glycan binding interactions for five cultured human cancer cell lines as assessed by glycan array analysis in the presence of 4-guanidino-Neu5Ac2en.

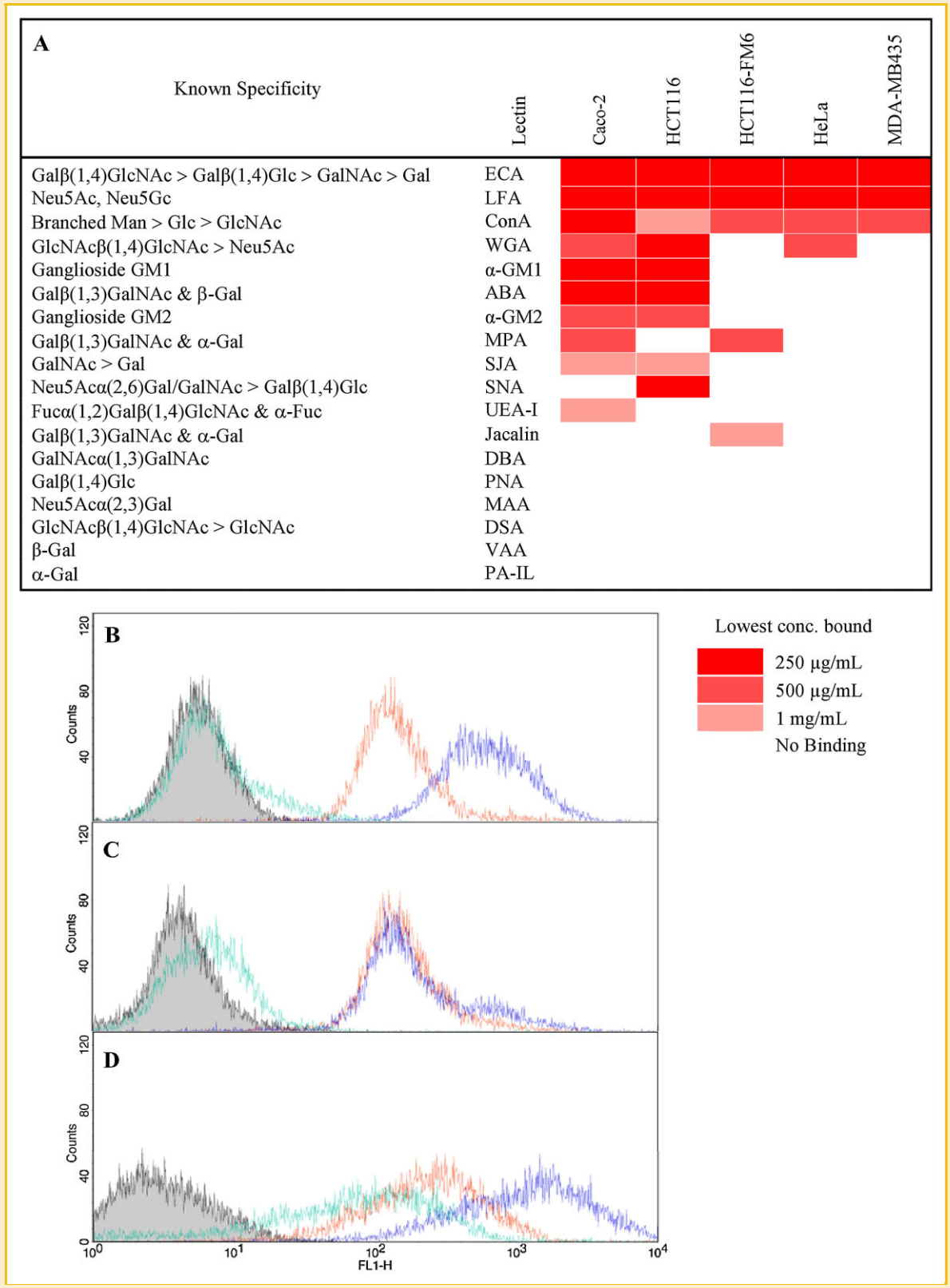

Fig. 3. Lectin array and flow cytometry analysis of human cancer cell lines. Diagrammatic representation depicting significant binding to lectins of various glycan specificities by five cultured human cancer cell lines (A). Flow cytometry analysis of Caco-2 (B), HeLa (C) and HCT116 (D) cells labelled with FITC conjugated SNA (green line), ECA (blue line) and ConA (red line).

printing of ABA and anti-GM1 at high-density influences their binding capacity, probably through changes in lectin/antibody conformational induced by overcrowding. Binding to anti-GM2 was also observed.

HCT116 cells showed strongest binding to ECA in a manner dependent on the concentration of lectin printed, showing that there is a high presence of terminal LacNAc structures (Fig. 8, Supplementary Material). Significant binding to all concentrations of LFA, as well as WGA was also observed, suggesting the presence of terminal Sia residues. Interaction, although relatively weak, to SNA indicates that Sia may occur α2,6-linked. Other significant interactions to ConA, SJA and anti-GM2 were also observed but only at the highest concentrations printed (Fig. 12, Supplementary Material). As observed for Caco-2 cells, binding to ABA and anti-GM1was only observed at 250 μg/ml.

In comparison to HCT116 cells, the MUC-1 expressing HCT116–FM6 had dramatically altered cell surface glycosylation pattern, with binding predominantly restricted to ECA, LFA and ConA (Fig. 13, Supplementary Material). Of particular note was the lack of binding to anti-GM1 and anti-GM2, suggesting that the expression of MUC-1 may be masking underlying structures and thus hindering antibody access to gangliosides on the cell surface. Even though HCT116–FM6 interaction with LFA points to the presence of terminal Sia, the lack of binding to WGA, SNA and MAA suggests that LFA may have a broader specificity than that reported in the literature. Similarly, three lectins, ABA, MPA and Jacalin, which are reported to recognise Galβ(1,3)GalNAc, were include on our array. However, only binding to MPA and Jacalin was noted for HCT116–FM6, indicating that perhaps binding of these lectins may be due to the presence of other listed binding specificities such as α-Gal structures (Fig. 3A).

The human cervical cancer cells HeLa and MDA-MB435 breast cancer cells exhibited the most defined pattern of cell surface glycosylation of the five cell lines analysed (Fig. 3). HeLa cells were bound by ECA, LFA, ConA and WGA (Fig. 14, Supplementary Material). MDA-MB435 bound a similar sub-set of lectins, with the exception of WGA, which was not recognised (Fig. 15, Supplementary Material).

To validate the lectin array data, Caco-2, HeLa and HCT116 cells were selected for by flow cytometric analysis using FITC-labelled SNA, ConA and ECA lectins (Fig. 3B, C and D). Flow cytometric analysis correlated well with our lectin array screening, with significant binding observed with FITC-labelled ConA and ECA to all three cell lines. Little or no binding was detected for Caco-2 and HeLa cells probed with FITC-labelled SNA, whereas SNA binding to HCT116 was observed, which again correlates well with our lectin array data.

DISCUSSION

In this study we employed glycan and lectin array technology to investigate any potential differential glycan binding or surface glycosylation signatures of five cell lines. To the best of our knowledge this is the first systematic study simultaneously investigating both the glycan binding specificity and the cell surface glycosylation of commonly used immortalised cell lines. Due to this unique perspective we were able to identify a clear relationship between the number of glycans bound by individual cell lines, and the diversity of glycans expressed on the cell surface. This relationship was best highlighted for MDA-MB435 cells, which bound the largest subset of glycan structures (Figs. 1 and 2), but had the least diverse surface glycans structures identified by lectin array analysis (Fig. 3). Conversely Caco-2 cells interacted with the least number of glycan structures (Figs. 1 and 2) but bound the largest subset of lectins inferring greater variety of cell surface glycans (Fig. 3). This inverse relationship between glycan and lectin array binding also held true for HeLa and HCT116 cell lines, with these cell lines possessing glycan binding and surface glycosylation signatures somewhere between that observed for Caco-2 and MDA-MB435 cells.

Interestingly, HCT116–FM6 cells bound to a more diverse number of glycans, and was recognised by a smaller number of lectins than wild-type HCT116 cells. The differential binding observed on our glycan array may reflect potential glycan–glycan interactions between the highly glycosylated MUC1 and glycans on the array. The differential results observed on our lectin array may be due to one of two factors. The expression of MUC1, which is predominantly *O*-glycosylated with terminal Gal and sialic acid structures, may be obscuring other glycans that would normally be exposed on the plasma membrane. Alternatively, MUC1 when bound by immobilised lectin on the array may lead to MUC1 being shed from the cell surface. MUC1 is known to act as a decoy receptor in pathogenic infection [McAuley et al., 2007] where the binding of a pathogen induces the release of MUC1 from the cell surface. We hypothesise that this may be occurring in the HCT116–FM6 MUC1-expressing cell line when bound with lectins that recognise common glycans present on MUC1 under normal glycosylation conditions [Patton et al., 1995].

Another significant observation was the absence of binding by cells of colonic origin to carrageen glycans and glycosaminoglycan (GAG) disaccharide sub-units (12A–13E). Only the MUC1-expressing HCT116–FM6 cells interacted with these structures, however all cell lines tested bound various hyaluronan structures (13N–14I). The latter is an expected result given that hyaluronan is a widely expressed GAG present in the extracellular matrix of almost all body tissues [Chakrabarti and Park, 1980; Toole, 1990].

Our unexpected initial finding that all cell lines with the exception of Caco-2 cells bound sialylated glycans led us to explore the possibility that the well-characterised plasma membrane neuraminidase Neu3 [Kakugawa et al., 2002; Miyagi et al., 2008] may be cleaving Sia from sialoglycoconjuagtes immobilised on our array, thus exposing the sub-terminal sugar. The addition of the influenza virus sialidase inhibitor (4-deoxy-4-guanidino-Neu5Ac2en) to our glycan array eliminated all putative interaction to sialoglycoconjuagtes, with the exception of MDA-MB435's interaction with sialyl-lewis A (10A). This interaction to the best of our knowledge has not been previously reported. Importantly, our study highlights the significance of inhibiting Neu3 activity when investigating the glycan binding potential of live cells by glycan array analysis.

The analysis of glycosylation signatures on live cells including Caco-2 and HeLa cells using lectin array technology has been

reported [Tao et al., 2008]. However, the glycosylation signatures observed for Caco-2 and HeLa cells in our study varies significantly to that previously reported. Of the 15 commercially available lectins used on our array, 14 of these were used on the Tao et al. lectin array. We found that Caco-2 cells showed significant binding to ECA, LFA, ConA, WGA, ABA, MPA and SJA. This was not observed by Tao et al. The only common interaction of Caco-2 cells on both arrays was to UEA-I. Similarly, we observed binding of HeLa cells to ECA, LFA and WGA that was not observed by Tao et al. In addition, Tao et al. reported HeLa binding to DBA, SJA, SNA and Jacalin that was likewise not observed in our study. In fact the only common interaction of HeLa cells on both arrays was to ConA. The unique interaction of ConA to Caco-2 cells and ECA to HeLa cells was confirmed by flow cytometry analysis (Fig. 3), thus verifying that our results were not false positives. The lack of binding of Caco-2 and HeLa cells to LFA and to a lesser extent WGA on the Tao et al. lectin array is particularly interesting given that both cell-lines are known to be heavily sialylated [Dennis et al., 1982]. However, we have noted variation in Sia binding between different batches of commercially available LFA (unpublished data), and this may in part explain the differences observed between the two studies.

What is clearly evident from the comparison of glycosylation signatures generated in our study and that previously reported [Tao et al., 2008] is that the glycosylation status of commonly used cell lines cultured in different laboratories varies significantly. Many factors may influence the glycans displayed on cell surfaces, including sugar concentration in the growth media [Hossler et al., 2009], passage number [Coughlan and Breen, 1995], cell density [Senechal et al., 1983; Coughlan and Breen, 1995] and the serum used [Hossler et al., 2009]. Given that changes in cell surface glycosylation may significantly impact on the validity of data generated from cell-based assays using common laboratory cell lines, we suggest that regular evaluation of glycosylation signatures be undertaken, either using lectin array technology or flow cytometry.

ACKNOWLEDGMENTS

NXA is supported by an Australian Postgraduate Award, CJD is supported by a Griffith University Postdoctoral Research Fellowship. This work was funded in part by Griffith University.

REFERENCES

Apweiler R, Hermjakob H, Sharon N. 1999. On the frequency of protein glycosylation, as deduced from analysis of the SWISS-PROT database. Biochim Biophys Acta (BBA)-Gen Subj 1473:4–8.

Brattain MG, Fine WD, Khaled FM, Thompson J, Brattain DE. 1981. Heterogeneity of malignant cells from a human colonic carcinoma. Cancer Res 41:1751–1756.

Cailleau R, Olivé M, Cruciger Q. 1978. Long-term human breast carcinoma cell lines of metastatic origin: preliminary characterization. In Vitro Cell Dev Biol-Plant 14:911–915.

Chakrabarti B, Park JW. 1980. Glycosaminoglycans: structure and interaction. CRC Crit Rev Biochem 8:225–313.

Cornil I, Kerbel R, Dennis J. 1990. Tumor cell surface beta 1-4-linked galactose binds to lectin(s) on microvascular endothelial cells and contributes to organ colonization. J Cell Biol 111:773–781.

Coughlan CM, Breen KC. 1995. The control of sialyltransferase activity in tumor-cell lines derived from different tissues in multifactorial. FEBS Lett 369:260–262.

Day CJ, Tiralongo J, Hartnell RD, Logue C-A, Wilson JC, von Itzstein M, Korolik V. 2009. Differential carbohydrate recognition by *Campylobacter jejuni* strain 11168: influences of temperature and growth conditions. PLoS ONE 4:e4927.

Dennis J, Waller C, Timpl R, Schirrmacher V. 1982. Surface sialic acid reduces attachment of metastatic tumour cells to collagen type IV and fibronectin. Nature 300:274–276.

Dennis JW, Granovsky M, Warren CE. 1999. Glycoprotein glycosylation and cancer progression. Biochim Biophys Acta (BBA)-Gen Subj 1473: 21–34.

Hakomori S. 2002. Glycosylation defining cancer malignancy: new wine in an old bottle. Proc Natl Acad Sci USA 99:10231–10233.

Hartley-Tassell LE, Shewell LK, Day CJ, Wilson JC, Sandhu R, Ketley JM, Korolik V. 2010. Identification and characterization of the aspartate chemosensory receptor of Campylobacter jejuni. Mol Microbiol 75:710–730.

Hata K, Koseki K, Yamaguchi K, Moriya S, Suzuki Y, Yingsakmongkon S, Hirai G, Sodeoka M, von Itzstein M, Miyagi T. 2008. Limited inhibitory effects of oseltamivir and zanamivir on human sialidases. Antimicrob Agents Chemother 52:3484–3491.

Hirabayashi J. 2003. Oligosaccharide microarrays for glycomics. Trends Biotechnol 21:141–143.

Hirabayashi J, Hashidate T, Arata Y, Nishi N, Nakamura T, Hirashima M, Urashima T, Oka T, Futai M, Muller WEG, Yagi F, Kasai K-i. 2002. Oligosaccharide specificity of galectins: a search by frontal affinity chromatography. Biochim Biophys Acta (BBA)-Gen Subj 1572:232–254.

Hossler P, Khattak SF, Li ZJ. 2009. Optimal and consistent protein glycosylation in mammalian cell culture. Glycobiology 19:936–949.

Iozzo RV, Cohen I. 1993. Altered proteoglycan gene expression and the tumor stroma. Cell Mol Life Sci 49:447–455.

Jones HWJ, Mc Kusick VA, Harper PS, Wuu K-D. 1971. GEORGE OTTO GEY (1899-1970): the HeLa cell and a reappraisal of its origin. Obstet Gynecol 38:945–949.

Jumarie C, Malo C. 1991. Caco-2cells cultured in serum-free medium as a model for the study of enterocytic differentiation in vitro. J Cell Physiol 149:24–33.

Kakugawa Y, Wada T, Yamaguchi K, Yamanami H, Ouchi K, Sato I, Miyagi T. 2002. Up-regulation of plasma membrane-associated ganglioside sialidase (Neu3) in human colon cancer and its involvement in apoptosis suppression. Proc Natl Acad Sci USA 99:10718–10723.

Liang P-H, Wu C-Y, Greenberg WA, Wong C-H. 2008. Glycan arrays: biological and medical applications. Curr Opin Chem Biol 12:86–92.

McAuley JL, Linden SK, Png CW, King RM, Pennington HL, Gendler SJ, Florin TH, Hill GR, Korolik V, McGuckin MA. 2007. MUC1 cell surface mucin is a critical element of the mucosal barrier to infection. J Clin Invest 117: 2313–2324.

Miyagi T, Wada T, Yamaguchi K. 2008. Roles of plasma membrane-associated sialidase NEU3 in human cancers. Biochim Biophys Acta 1780:532–537.

Patton S, Gendler SJ, Spicer AP. 1995. The epithelial mucin, MUC1, of milk, mammary gland and other tissues. Biochim Biophys Acta (BBA)-Rev Biomembr 1241:407–423.

Ross DT, Scherf U, Eisen MB, Perou CM, Rees C, Spellman P, Iyer V, Jeffrey SS, Van de Rijn M, Waltham M, Pergamenschikov A, Lee JC, Lashkari D, Shalon D, Myers TG, Weinstein JN, Botstein D, Brown PO. 2000. Systematic

variation in gene expression patterns in human cancer cell lines. Nat Genet 24:227–235.

Senechal H, Delain D, Schapira G, Wahrmann JP. 1983. Alterations in glycosylation of plasma membrane proteins during myogenesis. Exp Cell Res 147:341–350.

Song X, Xia B, Stowell SR, Lasanajak Y, Smith DF, Cummings RD. 2009. Novel fluorescent glycan microarray strategy reveals ligands for galectins. Chem Biol 16:36–47.

Tao S-C, Li Y, Zhou J, Qian J, Schnaar RL, Zhang Y, Goldstein IJ, Zhu H, Schneck JP. 2008. Lectin microarrays identify cell-specific and functionally significant cell surface glycan markers. Glycobiology 18:761–769.

Toole BP. 1990. Hyaluronan and its binding proteins, the hyaladherins. Curr Opin Cell Biol 2:839–844.

Wells L, Hart GW. 2003. O-GlcNAc turns twenty: functional implications for post-translational modification of nuclear and cytosolic proteins with a sugar. FEBS Lett 546:154–158.